
Class-Attentive Diffusion Network for Semi-Supervised Classification

Jongin Lim¹ Daeho Um¹ Hyung Jin Chang² Dae Ung Jo¹ Jin Young Choi¹

¹ Department of ECE, ASRI, Seoul National University
{ljin0429, daehoum1, mardaewoon, jychoi}@snu.ac.kr

² School of Computer Science, University of Birmingham
h.j.chang@bham.ac.uk

Abstract

We propose Aggregation with Class-Attentive Diffusion (AggCAD), a novel aggregation scheme for semi-supervised classification on graphs, which enables the model to embed more favorable node representations for better class separation. To this end, we propose a novel Class-Attentive Diffusion (CAD) which strengthens attention to intra-class nodes and attenuates attention to inter-class nodes. In contrast to the existing diffusion methods with a transition matrix determined solely by the graph structure, CAD considers both the node features and the graph structure with the design of the class-attentive transition matrix which utilizes the classifier. In addition, we further propose an adaptive scheme for AggCAD that leverages different reflection ratios of the diffusion result for each node depending on the local class-context. As the main advantage, AggCAD alleviates the problem of undesired mixing of inter-class features caused by discrepancies between node labels and the graph structure. Built on AggCAD, we construct *Class-Attentive Diffusion Network* for semi-supervised classification. Comprehensive experiments demonstrate the validity of AggCAD and the results show that the proposed method significantly outperforms the state-of-the-art methods on three benchmark datasets.

1 Introduction

Semi-supervised learning is a long-standing problem in machine learning. Many semi-supervised learning algorithms rely on the geometry of the data induced by both labeled and unlabeled data points [6]. Since this geometry can be naturally represented by a graph whose nodes are data points and edges represent relations between data points, graph-based semi-supervised learning has been extensively studied for decades [4, 18, 44, 48, 50]. In this paper, we focus on the problem of semi-supervised node classification that, given a graph in which only partial nodes are labeled, the aim is to infer the class of those unlabeled nodes.

Graph Neural Networks (GNNs) have achieved remarkable progress in this field recently [41, 47, 49]. In particular, [13, 18] have received great attention due to its flexibility and good performances. Underlying these methods is a neighborhood aggregation (or “message passing” [11]) which forms a new representation of a node by aggregating features of itself and its neighbors. The neighborhood aggregation is essentially a type of Laplacian smoothing [34], i.e., making the features of neighboring nodes similar [7, 23], which makes the subsequent classification task easier. Built on this, several methods have developed the weighted aggregation using attention mechanisms [35, 37, 46] where the weighting coefficients are determined by the features of each neighboring node pair.

One of the fundamental weaknesses with neighborhood aggregation methods is the lack of ability to capture long-range dependencies caused by over-smoothing [7, 19, 23, 43]. When stacking multiple

layers to expand their range, the diameter of the smoothed area grows large, and eventually, the node representations in the entire graph become indistinguishable. Although there have been miscellaneous efforts to overcome this issue [2, 38, 43], the range of these methods is still limited. Therefore, it is desirable to have the ability to propagate the label information over long-range, especially for large graphs or under sparsely labeled settings.

In recent literature, diffusion-based methods [3, 15, 19, 20] have demonstrated the capability of capturing long-range dependencies without leading to over-smoothing. These methods utilize graph diffusion as an alternative to neighborhood aggregation. Graph diffusion is a Markov process which spreads the information from the node to the adjacent nodes at each time step [25, 27]. Theoretically, K -steps of feature diffusion means that features of up to K -hop neighbors are aggregated to each node. This aggregation-by-diffusion scheme allows the model to achieve a larger range without changing the neural network [19], whereas in the neighborhood aggregation scheme expanding the range would require additional layers. However, a major limitation of these methods is that they only utilize the graph structure with a transition matrix of diffusion determined by the adjacency matrix. Since edges in real graphs are often noisy [16, 20] and could contain additional information [18], there exist discrepancies between node labels and the graph structure [7], i.e., some nodes may have more inter-class neighbors. Thus, the aggregation scheme determined solely by the graph structure may lead to corrupted representations due to the inter-class connections.

To address the aforementioned limitation, we propose Aggregation with Class-Attentive Diffusion (AggCAD), a new aggregation scheme which attentively aggregate nodes probably of the same class among K -hop neighbors. The proposed AggCAD consists of two steps. First, the aggregated feature representations are obtained by means of a novel Class-Attentive Diffusion (CAD) which strengthens attention to intra-class nodes and attenuates attention to inter-class nodes by considering the node features as well as the graph structure. Second, AggCAD forms the final feature representation of a node by linearly interpolating the node’s feature and the aggregated feature by CAD where the reflection ratio of the aggregated feature is adjusted differently for each node depending on its local class-context, i.e., if a node has many inter-class neighbors, AggCAD puts more weights on the node’s feature to preserve it and vice versa. Built on AggCAD, we construct a simple model for semi-supervised classification called *Class-Attentive Diffusion Network* and show that AggCAD enables the model to embed more favorable feature representations for better class separation. We validate the proposed method through extensive experiments and demonstrate that it significantly outperforms the state-of-the-art methods on three benchmark datasets.

2 Related Work

2.1 Graph Neural Networks

In recent literature on GNNs, there are two mainstreams: spectral-based methods and spatial-based methods. The spectral-based methods [5, 8, 14, 18] developed graph convolutions in the spectral domain using the graph Fourier transform or its extensions. However, these methods do not scale well with large graphs due to the computational burden. The spatial-based methods [11, 13, 24, 28, 29, 37], on the other hand, defined convolution-like operations directly on the graph. The spatial-based methods, in particular, the neighborhood aggregation scheme [11, 13, 18] have received considerable attention recently due to its efficiency and superior performance. Built on the neighborhood aggregation, numerous variants have been proposed. In the following, we categorize recent methods into three groups based on what they leverage to improve the model.

(i) *Extended Aggregation*. In [2], features aggregated from neighbors at different hops are concatenated before each layer, while in [43], skip connections are exploited to *jump* knowledge to the last layer. In [38], multi-layers of graph convolutions [18] are simplified into a single layer using the K -th power of an adjacency matrix, which means that the aggregation extends to the K -hop neighbor. These methods use an extended neighborhood for aggregation. However, the range of these methods is still limited, attributed to the low number of layers used.

(ii) *Feature Attention*. Attention-based methods [35, 37, 46] have utilized attention mechanisms to develop weighted aggregation where the weighting coefficients are determined by the features of each neighboring node pair. However, the aggregation of these methods is still limited to 1-hop neighbor. Meanwhile, [10] proposed graph pooling and unpooling operations based on feature attention and then, developed an encoder-decoder architecture in analogy to U-Net [32]. However, the pooling

operation proposed in their method does not take the graph structure into account but only depends on the node features [22].

(iii) *Graph Diffusion*. Recently, there have been several promising attempts by utilizing graph diffusion. These methods aggregate features by propagation over nodes using random walks [3, 26, 45], Personalized PageRank (PPR) [19], Heat Kernel (HK) [42], regularized Laplacian smoothing-based diffusion methods [15]. Meanwhile, [20] utilizes generalized graph diffusion (e.g. PPR and HK) to generate a new graph, then use this new graph instead of the original graph to improve performance. However, all of these methods do not take node features into account in their diffusion.

2.2 Random Walks on Graph

Random walks have been extensively studied in classical graph learning; see [25, 27] for an overview of existing methods. In particular, random walks were used in the field of unsupervised node embedding [1, 12, 31, 36]. Unlike these methods, the proposed method aims to embed a more favorable node representation for semi-supervised classification. To achieve this, the proposed diffusion is class-attentive by considering the node features as well as the graph structure, while in those methods, it only depends on the graph adjacency matrix. In [39, 40], Partially Absorbing Random Walk (PARW), a second-order Markov chain with partial absorption at each state, was proposed for semi-supervised learning. However, the state distribution of PARWs is also determined solely by the graph structure. The novelty of the proposed method is to design class-attentive diffusion by incorporating both the node features and the graph structure.

3 Proposed Method

3.1 Problem Setup

Formally, the problem of semi-supervised node classification considers a graph $G = (\mathcal{V}, \mathcal{E}, X)$ where $\mathcal{V} = \{v_i\}_{i=1}^N$ is the set of N nodes, \mathcal{E} denotes the edges between nodes, and $X \in \mathbb{R}^{N \times D}$ is a given feature matrix, i.e., x_i , i -th row of X , is D -dimensional feature vector of the node v_i . Since edge attributes may not be given, we consider unweighted version of the graph represented by an adjacency matrix $A = [a_{ij}] \in \mathbb{R}^{N \times N}$ where $a_{ij} = 1$ if $\mathcal{E}(i, j) \neq 0$ and $a_{ij} = 0$ otherwise. We denote the given label set as Y_L associated with the labeled node set \mathcal{V}_L , i.e., $y_i \in Y_L$ be a one-hot vector indicating one of C classes for v_i . We focus on the transductive setting [18, 44] which aims to infer the labels of the remaining unlabeled nodes based on (X, A, Y_L) .

In general, the model for semi-supervised node classification can be expressed as

$$Z = f_\theta(X, A) \quad \text{and} \quad \hat{y}_i = g_\phi(z_i) \quad (i = 1, 2, \dots, N) \quad (1)$$

where f_θ is a feature embedding network to embed the feature representations Z from (X, A) , and g_ϕ is a node classifier predicting \hat{y}_i from z_i , i -th row of Z . The feature embedding network f_θ is realized by a GNN architecture in recent literature. The process of GNN can be decomposed into two steps: feature transformation and feature aggregation, where the former stands for a non-linear transformation of node features and the latter refers to the process of forming new node feature representations via aggregating proximal node features.

In this paper, we focus on the process of feature aggregation. More specifically, we aim to design an aggregation scheme which can be applied before the classifier from Eq. (1) to embed more favorable feature representations for class separation (i.e., given feature representations $Z \in \mathbb{R}^{N \times F}$, the aim is to form new representation denoted by $Z^{(\text{AggCAD})} \in \mathbb{R}^{N \times F}$ for better classification). To achieve this, we design Aggregation with Class-Attentive Diffusion (AggCAD), a novel aggregation scheme defined as,

$$Z^{(\text{AggCAD})} \leftarrow \text{AggCAD}(Z, A, \{g_\phi(z_i)\}_{i=1}^N). \quad (2)$$

The key insight of AggCAD is to attentively aggregate nodes probably of the same class among K -hop neighbors to make the feature representations of the same class become similar. Since the true class likelihood distribution is intractable, we exploit the classifier to approximate the class likelihood of the node v_i as $g_\phi(z_i)$. In contrast to attention-based methods [35, 37, 46], or diffusion-based methods [3, 15, 19, 20], the node features Z , the graph structure A , and the class information are jointly utilized. In Section 3.2, we present the proposed AggCAD in detail. Then, we introduce *Class-Attentive Diffusion Network*, a simple model based on AggCAD in Section 3.3.

3.2 Aggregation with Class-Attentive Diffusion

For clarity, we first describe how AggCAD works on each node, and present the overall formula in a matrix form. The proposed AggCAD forms a new feature representation of a node v_i as follows,

$$z_i^{(\text{AggCAD})} = (1 - \gamma_i)z_i + \gamma_i \sum_{j \in \mathcal{N}_K(i)} \alpha_{ij} \cdot z_j. \quad (3)$$

where $\mathcal{N}_K(i)$ denotes K -hop neighbors of v_i . The key components of AggCAD are α_{ij} and γ_i where α_{ij} is attention parameter for each node feature z_i , which sums to 1 (i.e., $\sum_j \alpha_{ij} = 1$), and $\gamma_i \in [0, 1]$ is another attentive parameter which adaptively controls the importance between its own feature and the aggregated feature depending on the local class-context. Note that both α_{ij} and γ_i depend on (Z, A, g_ϕ) . In the following, we describe the detailed designs for α_{ij} and γ_i .

Design of α_{ij} . The design objective for α_{ij} is to strengthen attention to intra-class nodes and attenuate attention to inter-class nodes among K -hop neighbors. To achieve this, we propose Class-Attentive Diffusion (CAD), a novel stochastic process which combines the advantages of both the attention mechanism and the random walk process. The proposed CAD consists of N Class-Attentive Random Walks (CARWs) starting at each node in the graph. Suppose a CARW that starts from the node v_i , the CARW determines the next node among the neighbor by comparing the class likelihood distributions given the node features, i.e., comparing $\mathbf{p}_i = p(y_i|z_i)$ and $\mathbf{p}_j = p(y_j|z_j)$ for $j \in \mathcal{N}(i)$. The more similar \mathbf{p}_i and \mathbf{p}_j , the more likely the CARW moves from v_i to v_j . To this end, we define the transition probability from v_i to v_j as

$$T_{ij} = \text{softmax}_{j \in \mathcal{N}(i)}(\mathbf{p}_i^T \mathbf{p}_j). \quad (4)$$

Note that, \mathbf{p}_i is a categorical distribution of which c -th element $\mathbf{p}_i(c)$ is the probability of node i belongs to class c . Thus, the cosine distance between \mathbf{p}_i and \mathbf{p}_j (i.e., $\mathbf{p}_i^T \mathbf{p}_j$) can be one possible solution for measuring the similarity between them. However, the true distribution \mathbf{p}_i is intractable. Instead, we approximate the distribution by exploiting the classifier g_ϕ in Eq. (1) where the probability of each class is inferred by g_ϕ based on the node feature z_i . That is,

$$\mathbf{p}_i \approx p(\hat{y}_i|z_i) = g_\phi(z_i). \quad (5)$$

As the learning progresses, the transition matrix in Eq. (4) gradually becomes more class-attentive by means of g_ϕ . This is the key difference from the diffusion-based methods [3, 15, 19, 20] where the transition matrix is only determined by the adjacency matrix.

Then, the row vector $\pi_i^{(t)} \in \mathbb{R}^N$, the state distribution of the CARW after t steps, is derived by $\pi_i^{(t+1)} = \pi_i^{(t)} T$. For large enough K , $\pi_i^{(K)}(j)$ reflects the importance scores of v_j on v_i as it grows with the similarity \mathbf{p}_i and \mathbf{p}_j . Therefore, it is natural to design as follows,

$$\alpha_{ij} = \pi_i^{(K)}(j). \quad (6)$$

Design of γ_i . Now, we introduce how to design γ_i to control the trade-off between its own node feature z_i and the aggregated feature by the proposed diffusion $\sum_j \alpha_{ij} z_j$ by considering the local class-context. We first introduce our motivation. In real graphs, some nodes may be connected to nodes of various classes, or even worse, nodes of the same class may not even exist in their neighbors. Intuitively, in these cases, γ_i should be adjusted to a small value to preserve its original feature and avoid undesired smoothing. Conversely, for nodes with neighbors of the same class, γ_i should be larger to accelerate proper smoothing. Motivated by this, we define a control variable c_i as follows,

$$c_i = \frac{1}{\text{deg}(i)} \sum_{j \in \mathcal{N}(i)} g_\phi(z_i)^T g_\phi(z_j), \quad (7)$$

where $\text{deg}(i)$ is the degree of v_i and g_ϕ is the aforementioned classifier. Then, the range of c_i would be $0 \leq c_i \leq 1$. The meaning of c_i is that the more nodes of the same class in the neighborhood, the greater the value of c_i and vice versa. Hence the larger c_i , the higher the confidence on the diffusion result and thus γ_i should be proportional to c_i . To this end, we set up an adaptive formula for γ_i as

$$\gamma_i = (1 - \beta)c_i + \beta\gamma_u \quad (8)$$

where $\gamma_u = 1$ is the upper bound of γ_i to keep $0 \leq \gamma_i \leq 1$ for interpolation of each node feature and the diffusion result. As a result, γ_i divides c_i and 1 internally in the ratio of $\beta : (1 - \beta)$ where

$\beta \in [0, 1]$ controls the sensitivity of how much γ_i will be adjusted according to c_i . In this work, the sensitivity β is determined empirically for each dataset since different graphs exhibit different neighborhood structures [1, 19].

Matrix Form. Now, we present the overall formula of AggCAD in a matrix form. By letting $\mathbf{\Gamma} = \text{diag}(\gamma_1, \gamma_2, \dots, \gamma_N)$ and $\mathcal{A} = (\alpha_{ij}) \in \mathbb{R}^{N \times N}$, Eq. (3) can be trivially extended to the entire graph and expressed by a matrix form as

$$Z^{(\text{AggCAD})} = (\mathbf{I} - \mathbf{\Gamma}) \cdot Z + \mathbf{\Gamma} \cdot \mathcal{A} \cdot Z. \quad (9)$$

Note that AggCAD preserves the graph’s sparsity and never needed to construct an $\mathbb{R}^{N \times N}$ matrix. Instead, the second term in Eq. (9) can be implemented by K -steps of diffusion as in [19]. Further, since we utilize the classifier g_ϕ , AggCAD does not require additional learning parameters.

3.3 Class-Attentive Diffusion Network

Built on the proposed AggCAD, we construct *Class-Attentive Diffusion Network* (CAD-Net) for semi-supervised classification. CAD-Net consists of the feature embedding network f_θ followed by AggCAD and the classifier g_ϕ as defined in Eq. (1), (2) and (9). More specifically, we realize f_θ with 2-layers of MLP for simplicity, as the process of feature aggregation can be sufficiently performed in AggCAD, and g_ϕ is realized by the softmax function, i.e., $\hat{y}_i = g_\phi(z_i) = \text{softmax}(z_i)$ as in other literature [15, 18, 19, 38], and thus the dimension of node feature z_i is set to the number of classes. The whole network parameters can then be trained in an end-to-end manner by minimizing the cross-entropy loss function \mathcal{L}_{sup} over all labeled nodes. By minimizing the cross-entropy between the label y_i , a one-hot vector indicating one of C classes, and the prediction \hat{y}_i for all $y_i \in Y_L$, the model can be learned to enhance the element of z_i , corresponding to the index that indicates the class of y_i , which facilitates the class separation. In addition to \mathcal{L}_{sup} , we consider another regularization objective. In AggCAD, the transition matrix of CAD is determined by \mathbf{p}_i as defined in Eq. (4) and (5). The initial class likelihood distribution \mathbf{p}_i for each node should generally be close to a one-hot vector such that the resulting transition matrix becomes more class-attentive. Thus, we regularize the entropy of \mathbf{p}_i by minimizing $\mathcal{L}_{\text{ent}} = \sum_{i=1}^N H(\mathbf{p}_i)$ where H denotes the entropy function. During training, \mathcal{L}_{sup} and \mathcal{L}_{ent} are jointly minimized by using Adam optimizer [17]. We report the detailed implementation in Appendix A.

4 Experiments

4.1 Experimental Setup

Datasets. To validate the proposed method, we utilized three benchmark datasets (CiteSeer, Cora, and PubMed) [33]. These are citation networks where each node represents a document and each edge represents a citation link between two documents. For each node, bag-of-words representation whose dimension is determined by the dictionary size is given. We pre-processed the datasets by removing self-loops and duplicated edges from the graphs as in [9] and used these pre-processed versions of the graphs for all experiments. For evaluation, we closely followed the standard experimental setup suggested in [44]. There are 20 nodes per class for train, 500 nodes for validation, and 1000 nodes for test. For all experiments, we evaluated the average accuracy (%) computed over 100 independent runs. Statistics of datasets are reported in Appendix B.1.

Baselines. We compared the proposed method with 12 state-of-the-art methods which can be categorized into 4 groups: i) *Vanilla* = {Chebyshev convolution (Cheby) [8], Graph Convolutional Networks (GCN) [18], GraphSAGE (SAGE) [13]}, ii) *Extended Aggregation* = {Jumping Knowledge (JK) [43], MixHop [2], Simplifying GCN (SGC) [38]}, iii) *Feature Attention* = {Attention-based GNNs (AGNN) [35], Graph Attention Networks (GAT) [37], Graph U-Nets [10]}, and iv) *Graph Diffusion* = {Approximated Personalized PageRank for Neural Prediction (APPNP) [19], Graph Diffusion Convolution (GDC) [20], Graph Diffusion-Embedding Networks (GDEN) [15]}. For a fair comparison, we used the publicly released codes. For GDEN [15], we report the performance taken from their paper since the code is not available.

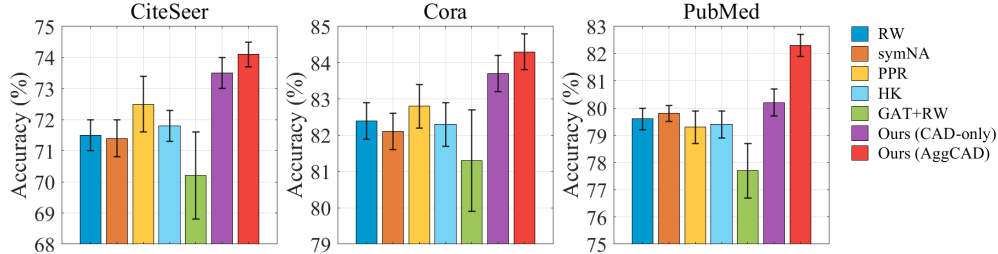


Figure 1: Accuracy with different aggregation methods. Note that only the aggregation part is switched from the same CAD-Net architecture. Our variants show superior results for all datasets.

4.2 Validity of AggCAD

Comparison with Different Aggregation Methods. To verify the effectiveness of AggCAD, we compared AggCAD with 6 different aggregation methods. For a fair comparison, only AggCAD is replaced by different aggregation methods in the same CAD-Net architecture. Firstly, we consider assorted diffusion methods including Random Walks (RW), symmetric Normalized Adjacency matrix (symNA), Personalized PageRank (PPR) [30], and Heat Kernel (HK) [21]. For RW and symNA, the transition matrix is defined as $D^{-1}A$ and $D^{-\frac{1}{2}}AD^{-\frac{1}{2}}$ respectively, and we proceed K -steps of feature diffusion according to their transition matrix. For PPR and HK, the closed-form solution of the diffusion state distribution is used as in [15, 19, 20]. Secondly, we construct GAT+RW, an attentive diffusion based on GAT [37]. In GAT+RW, the transition matrix is defined by the attention value computed by GAT, and we proceed K -steps of feature diffusion according to it. Lastly, we also consider CAD-only, which only uses CAD via α without the adaptive aggregation by γ in AggCAD.

Figure 1 shows the overall comparisons with the aforementioned variants. Compared to RW, sym, PPR, and HK, which only utilize the graph structure, our variants (CAD-only and AggCAD) show superior results. The better performance comes from the proposed class-attentive transition matrix both utilizing node features and the graph structure. While GAT+RW can utilize both node features and the graph structure as an attentive diffusion method, its performance is not sufficient, which demonstrate the effectiveness of our design of class-attentive diffusion. The proposed AggCAD shows better performance than only using CAD, which demonstrate the effect of adaptive aggregation by γ . By means of γ , the model can adjust the reflection ratio of the diffusion to prevent corrupted representations from inter-class neighbors, which leads to better performance.

Learning Process. Figure 2 shows the cross-entropy loss on validation set of CiteSeer across different epochs. We compare the learning curve of CAD-Net with the aforementioned RW model. There is no difference from RW at the beginning, but CAD-Net obtains obviously lower cross-entropy loss values at convergence. It clearly demonstrates that the transition of CAD becomes gradually class-attentive as the learning progresses, which leads to better predictive accuracy of CAD-Net.

Influence of Different Hidden Units. Unlike attention-based methods [35, 37], the proposed CAD can be self-guided by the classifier without the need for additional parameters for attention. Thus, the total number of parameters can be implemented in the same way as the vanilla GCN [18]. To validate the effectiveness of AggCAD, we evaluated the performance across the different numbers of hidden units in the feature embedding network f_θ , and compared the results with GCN [18] and APPNP [19] which have the same number of parameters. As shown in Figure 3, CAD-Net shows robust performance with respect to the number of hidden units. Further, for all experiments, we can observe that CAD-Net significantly outperforms GCN and APPNP with the same number of parameters. This demonstrates that the superior performance of CAD-Net is attributed to the effect of the proposed AggCAD, not the power of the feature embedding network.

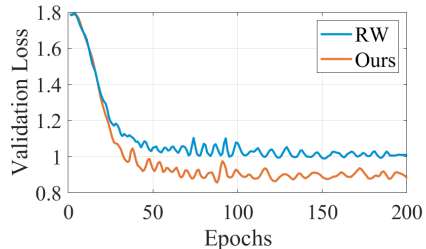


Figure 2: Validation loss across different epochs on CITESEER.

Table 1: Accuracy (%) under standard benchmark setting. The best results are marked by bold. We report the mean with the standard deviation (Mean \pm Std) computed over 100 independent runs. For GDEN [15], we report the performance taken from their paper.

Type	Method	CITESEER		CORA		PUBMED	
		Fixed	Random	Fixed	Random	Fixed	Random
Vanilla	Cheby [8]	70.7 \pm 0.5	69.1 \pm 1.9	81.4 \pm 0.5	77.8 \pm 2.3	75.2 \pm 1.4	73.1 \pm 3.2
	GCN [18]	71.1 \pm 0.7	68.3 \pm 1.9	81.3 \pm 0.7	79.3 \pm 1.8	79.0 \pm 0.5	77.2 \pm 2.6
	SAGE [13]	70.9 \pm 0.7	68.8 \pm 1.8	81.4 \pm 0.7	79.8 \pm 1.7	78.7 \pm 0.4	77.2 \pm 2.5
Extended Aggregation	JK [43]	69.1 \pm 1.1	67.5 \pm 1.9	81.2 \pm 0.8	78.6 \pm 1.9	78.7 \pm 0.5	77.7 \pm 2.7
	MixHop [2]	71.5 \pm 0.8	68.4 \pm 1.7	82.0 \pm 1.0	80.7 \pm 1.7	79.4 \pm 0.5	77.8 \pm 2.5
	SGC [38]	71.9 \pm 0.1	69.2 \pm 1.7	81.0 \pm 0.2	79.9 \pm 1.8	78.9 \pm 0.1	77.0 \pm 2.6
Feature Attention	AGNN [35]	71.5 \pm 0.7	69.4 \pm 1.8	82.8 \pm 0.6	80.8 \pm 1.8	79.3 \pm 0.8	78.0 \pm 2.4
	GAT [37]	72.5 \pm 0.8	70.0 \pm 1.9	83.1 \pm 0.8	81.6 \pm 1.5	79.0 \pm 0.3	77.3 \pm 2.4
	U-Nets [10]	70.2 \pm 1.0	67.9 \pm 1.9	82.9 \pm 0.7	81.2 \pm 1.9	78.0 \pm 0.5	77.8 \pm 2.6
Graph Diffusion	APPNP [19]	71.8 \pm 0.5	69.9 \pm 1.7	82.9 \pm 0.5	81.8 \pm 1.5	79.7 \pm 0.3	78.8 \pm 2.5
	GDC [20]	72.7 \pm 0.8	70.9 \pm 1.7	82.7 \pm 0.7	81.9 \pm 1.5	78.1 \pm 0.3	76.9 \pm 2.4
	*GDEN [15]	72.8	-	82.0	-	78.7	-
Proposed	CAD-Net	74.1 \pm 0.4	71.1 \pm 1.6	84.3 \pm 0.5	82.4 \pm 1.4	82.3 \pm 0.4	79.6 \pm 2.4

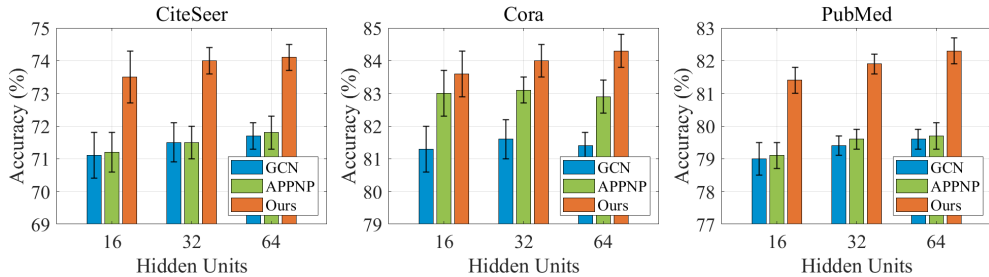


Figure 3: Accuracy with different numbers of hidden units. Note that GCN [18], APPNP [19], and the proposed CAD-Net have the same number of parameters. For all datasets, CAD-Net significantly outperform GCN and APPNP with the same number of parameters.

Influence of β . We also analyzed the influence of the hyperparameter β which controls the sensitivity of how much γ will be adjusted. While the optimum differs slightly for each dataset, we consistently found that any $\beta \in [0.65, 0.95]$ achieve the state-of-the-art performances. Due to the space limit, the results are reported in Appendix B.2. In addition, the distribution of the resulting γ values for entire nodes is also attached to Appendix B.2.

4.3 Comparison with State-of-the-art Methods

Evaluation on Benchmark Datasets. We evaluated the performances in two settings. First, we evaluated on *Fixed* train/validation/test split from [44]. We report the mean with the standard deviation computed over 100 independent runs. In addition, we also evaluated on 100 *Random* splits which randomly drawn dataset splits of the same size as in [44]. The overall results are reported in Table 1. In all experiments, the proposed CAD-Net shows superior performance to other methods. The better performance of CAD-Net comes from the proposed aggregation scheme based on the class-attentive diffusion (AggCAD) both utilizing node features and the graph structure in the transition matrix.

Influence of Different Label Rates. We then explored how the number of training nodes per class impacts the accuracy of the models. The ability to maintain robust performance even under very sparsely labeled settings is important. We compared the performances when the number of labeled nodes per class is changed to 20, 15, 10, and 5. The overall results are presented in Figure 4. Note that, the diffusion-based methods, APPNP [19] and GDC [20], do not show satisfactory results despite their wide range. This is because these methods only utilize the graph structure. In contrast, AggCAD aggregates nodes from a wide range and the importance of each node reflects both node features and the graph structure. As a result, the proposed CAD-Net shows robust and superior performance even under the very sparsely labeled setting and outperforms all other methods. Especially, the superiority

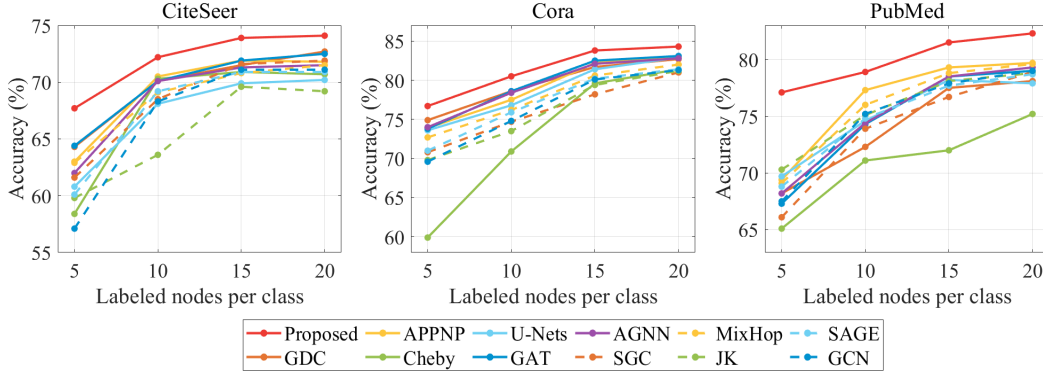


Figure 4: Accuracy with different numbers of labeled nodes per class. The proposed CAD-Net shows robust and superior performance for all settings.

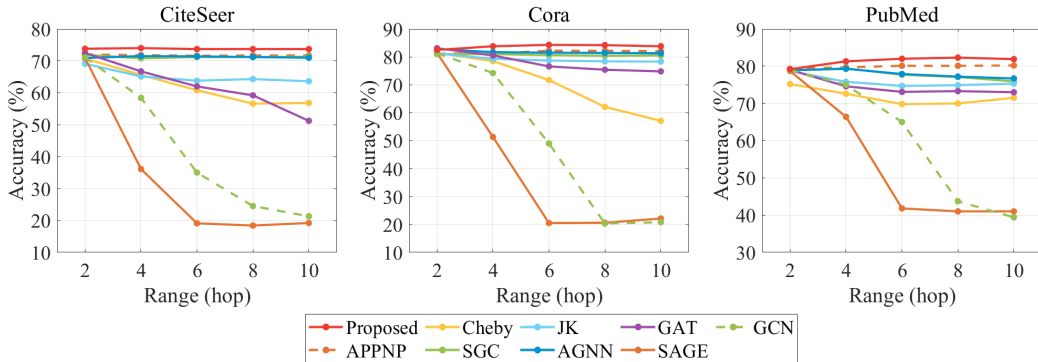


Figure 5: Accuracy with varying ranges of the model. The proposed CAD-Net shows superior performance regardless of the range. The dominance of CAD-Net increases for a longer range.

of CAD-Net is more obvious in PubMed which is a large dataset. This further demonstrates the effectiveness of AggCAD.

Influence of Different Ranges. Figure 5 shows how the accuracy depends on the different ranges. As expected, the neighborhood aggregation methods degrade performance with increasing layers. While the diffusion-based methods demonstrate the capability of capturing long-range dependencies, CAD-Net shows superior performance for all datasets. Also, as in the previous experiment, the superiority of CAD-Net is particularly evident in PubMed, which suggests that the proposed method is able to accommodate larger graphs or sparsely labeled settings. Detailed experimental setup and results in tabular form for Figure 4 and 5 are presented in Appendix B.2.

5 Conclusion

In this paper, we propose Aggregation with Class-Attentive Diffusion (AggCAD), a new aggregation scheme for semi-supervised classification on graphs. The main benefits of the proposed AggCAD are three aspects. (i) AggCAD attentively aggregates nodes probably of the same class among K -hop neighbors employing a novel Class-Attentive Diffusion (CAD). Unlike the existing diffusion methods, both the node features and the graph structure are leveraged in CAD with the design of the class-attentive transition matrix which utilizes the classifier. (ii) For each node, AggCAD adjusts the reflection ratio of the diffusion result differently depending on the local class-context, which prevents undesired mixing from inter-class neighbors. (iii) AggCAD does not require additional learning parameters since the class-attentive transition probability is defined by the classifier. The extensive experimental results demonstrate the validity of AggCAD illustrating that AggCAD enables the model to embed more favorable representations for better class separation. Class-Attentive Diffusion Network, our simple model based on AggCAD, achieves state-of-the-art performances by a large margin on CiteSeer, Cora, and PubMed datasets.

Broader Impact

Graphs, due to the strong representation ability, accommodate many potential applications in the real world, such as social networks, citation networks, web pages, etc. Our research is a study of neural networks applicable in the graph domain. Therefore, our research can be an important basis for graph-based applications to be applied in real life in the future. Besides, a large amount of cost is required to acquire high quality of labeled data. The problem of semi-supervised learning, which we focus on, can secure robust performance with a small number of labeled data, thus contributing to lowering the threshold of solving industrial or social problems using machine learning at a low cost.

Acknowledgments

We thank Tze Ho Elden Tse for the feedback. This work was supported by Institute for Information & communications Technology Promotion (IITP) grant funded by the Korea government (MSIP) (No.2017-0-00306, Outdoor Surveillance Robots) and ICT R&D program of MSIP/IITP (No.B0101-15-0552, Predictive Visual Intelligence Technology).

References

- [1] Abu-El-Haija, Sami, Perozzi, Bryan, Al-Rfou, Rami, and Alemi, Alexander A. Watch your step: Learning node embeddings via graph attention. In *Advances in Neural Information Processing Systems*, pp. 9180–9190, 2018. 3, 5
- [2] Abu-El-Haija, Sami, Perozzi, Bryan, Kapoor, Amol, Harutyunyan, Hrayr, Alipourfard, Nazanin, Lerman, Kristina, Steeg, Greg Ver, and Galstyan, Aram. Mixhop: Higher-order graph convolution architectures via sparsified neighborhood mixing. *arXiv preprint arXiv:1905.00067*, 2019. 2, 5, 7, 14
- [3] Atwood, James and Towsley, Don. Diffusion-convolutional neural networks. In *Advances in neural information processing systems*, pp. 1993–2001, 2016. 2, 3, 4
- [4] Belkin, Mikhail, Niyogi, Partha, and Sindhvani, Vikas. Manifold regularization: A geometric framework for learning from labeled and unlabeled examples. *Journal of machine learning research*, 7(Nov):2399–2434, 2006. 1
- [5] Bruna, Joan, Zaremba, Wojciech, Szlam, Arthur, and LeCun, Yann. Spectral networks and locally connected networks on graphs. *arXiv preprint arXiv:1312.6203*, 2013. 2
- [6] Chappelle, Olivier, Scholkopf, Bernhard, and Zien, Alexander. *Semi-supervised learning*. MIT Press, Cambridge, USA, 2006. 1
- [7] Chen, Deli, Lin, Yankai, Li, Wei, Li, Peng, Zhou, Jie, and Sun, Xu. Measuring and relieving the over-smoothing problem for graph neural networks from the topological view. *arXiv preprint arXiv:1909.03211*, 2019. 1, 2
- [8] Defferrard, Michaël, Bresson, Xavier, and Vandergheynst, Pierre. Convolutional neural networks on graphs with fast localized spectral filtering. In *Advances in neural information processing systems*, pp. 3844–3852, 2016. 2, 5, 7, 13, 14, 15
- [9] Fey, Matthias and Lenssen, Jan E. Fast graph representation learning with PyTorch Geometric. In *ICLR Workshop on Representation Learning on Graphs and Manifolds*, 2019. 5, 12
- [10] Gao, Hongyang and Ji, Shuiwang. Graph u-nets. *arXiv preprint arXiv:1905.05178*, 2019. 2, 5, 7, 14
- [11] Gilmer, Justin, Schoenholz, Samuel S, Riley, Patrick F, Vinyals, Oriol, and Dahl, George E. Neural message passing for quantum chemistry. In *Proceedings of the 34th International Conference on Machine Learning-Volume 70*, pp. 1263–1272. JMLR. org, 2017. 1, 2
- [12] Grover, Aditya and Leskovec, Jure. node2vec: Scalable feature learning for networks. In *Proceedings of the 22nd ACM SIGKDD international conference on Knowledge discovery and data mining*, pp. 855–864, 2016. 3

- [13] Hamilton, Will, Ying, Zhitao, and Leskovec, Jure. Inductive representation learning on large graphs. In *Advances in neural information processing systems*, pp. 1024–1034, 2017. [1](#), [2](#), [5](#), [7](#), [13](#), [14](#), [15](#)
- [14] Henaff, Mikael, Bruna, Joan, and LeCun, Yann. Deep convolutional networks on graph-structured data. *arXiv preprint arXiv:1506.05163*, 2015. [2](#)
- [15] Jiang, Bo, Lin, Doudou, Tang, Jin, and Luo, Bin. Data representation and learning with graph diffusion-embedding networks. In *Proceedings of the IEEE Conference on Computer Vision and Pattern Recognition*, pp. 10414–10423, 2019. [2](#), [3](#), [4](#), [5](#), [6](#), [7](#)
- [16] Khan, Arijit, Ye, Yuan, and Chen, Lei. On uncertain graphs. *Synthesis Lectures on Data Management*, 10(1):1–94, 2018. [2](#)
- [17] Kingma, Diederik and Ba, Jimmy. Adam: A method for stochastic optimization. *arXiv preprint arXiv:1412.6980*, 2014. [5](#), [12](#)
- [18] Kipf, Thomas N and Welling, Max. Semi-supervised classification with graph convolutional networks. *arXiv preprint arXiv:1609.02907*, 2016. [1](#), [2](#), [3](#), [5](#), [6](#), [7](#), [12](#), [13](#), [14](#), [15](#)
- [19] Klicpera, Johannes, Bojchevski, Aleksandar, and Günnemann, Stephan. Predict then propagate: Graph neural networks meet personalized pagerank. *arXiv preprint arXiv:1810.05997*, 2018. [1](#), [2](#), [3](#), [4](#), [5](#), [6](#), [7](#), [14](#), [15](#)
- [20] Klicpera, Johannes, Weissenberger, Stefan, and Günnemann, Stephan. Diffusion improves graph learning. In *Advances in Neural Information Processing Systems*, pp. 13333–13345, 2019. [2](#), [3](#), [4](#), [5](#), [6](#), [7](#), [12](#), [14](#)
- [21] Kondor, Risi Imre and Lafferty, John. Diffusion kernels on graphs and other discrete structures. In *ICML*, 2002. [6](#)
- [22] Lee, Junhyun, Lee, Inyeop, and Kang, Jaewoo. Self-attention graph pooling. *arXiv preprint arXiv:1904.08082*, 2019. [3](#)
- [23] Li, Qimai, Han, Zhichao, and Wu, Xiao-Ming. Deeper insights into graph convolutional networks for semi-supervised learning. In *Thirty-Second AAAI Conference on Artificial Intelligence*, 2018. [1](#)
- [24] Li, Yujia, Tarlow, Daniel, Brockschmidt, Marc, and Zemel, Richard. Gated graph sequence neural networks. *arXiv preprint arXiv:1511.05493*, 2015. [2](#)
- [25] Lovász, László et al. Random walks on graphs: A survey. [2](#), [3](#)
- [26] Ma, Zheng, Li, Ming, and Wang, Yuguang. Pan: Path integral based convolution for deep graph neural networks. *arXiv preprint arXiv:1904.10996*, 2019. [3](#)
- [27] Masuda, Naoki, Porter, Mason A, and Lambiotte, Renaud. Random walks and diffusion on networks. *Physics reports*, 716:1–58, 2017. [2](#), [3](#)
- [28] Monti, Federico, Boscaini, Davide, Masci, Jonathan, Rodola, Emanuele, Svoboda, Jan, and Bronstein, Michael M. Geometric deep learning on graphs and manifolds using mixture model cnns. In *Proceedings of the IEEE Conference on Computer Vision and Pattern Recognition*, pp. 5115–5124, 2017. [2](#)
- [29] Niepert, Mathias, Ahmed, Mohamed, and Kutzkov, Konstantin. Learning convolutional neural networks for graphs. In *International conference on machine learning*, pp. 2014–2023, 2016. [2](#)
- [30] Page, Lawrence, Brin, Sergey, Motwani, Rajeev, and Winograd, Terry. The pagerank citation ranking: Bringing order to the web. Technical report, Stanford InfoLab, 1999. [6](#)
- [31] Perozzi, Bryan, Al-Rfou, Rami, and Skiena, Steven. Deepwalk: Online learning of social representations. In *Proceedings of the 20th ACM SIGKDD international conference on Knowledge discovery and data mining*, pp. 701–710, 2014. [3](#)

- [32] Ronneberger, Olaf, Fischer, Philipp, and Brox, Thomas. U-net: Convolutional networks for biomedical image segmentation. In *International Conference on Medical image computing and computer-assisted intervention*, pp. 234–241. Springer, 2015. 2
- [33] Sen, Prithviraj, Namata, Galileo, Bilgic, Mustafa, Getoor, Lise, Galligher, Brian, and Eliassi-Rad, Tina. Collective classification in network data. *AI magazine*, 29(3):93–93, 2008. 5
- [34] Taubin, Gabriel. A signal processing approach to fair surface design. In *Proceedings of the 22nd annual conference on Computer graphics and interactive techniques*, pp. 351–358, 1995. 1
- [35] Thekumparampil, Kiran K, Wang, Chong, Oh, Sewoong, and Li, Li-Jia. Attention-based graph neural network for semi-supervised learning. *arXiv preprint arXiv:1803.03735*, 2018. 1, 2, 3, 5, 6, 7, 13, 14, 15
- [36] Tsitsulin, Anton, Mottin, Davide, Karras, Panagiotis, and Müller, Emmanuel. Verse: Versatile graph embeddings from similarity measures. In *Proceedings of the 2018 World Wide Web Conference*, pp. 539–548, 2018. 3
- [37] Veličković, Petar, Cucurull, Guillem, Casanova, Arantxa, Romero, Adriana, Lio, Pietro, and Bengio, Yoshua. Graph attention networks. *arXiv preprint arXiv:1710.10903*, 2017. 1, 2, 3, 5, 6, 7, 13, 14, 15
- [38] Wu, Felix, Zhang, Tianyi, Souza Jr, Amauri Holanda de, Fifty, Christopher, Yu, Tao, and Weinberger, Kilian Q. Simplifying graph convolutional networks. *arXiv preprint arXiv:1902.07153*, 2019. 2, 5, 7, 12, 13, 14, 15
- [39] Wu, Xiao-Ming, Li, Zhenguang, So, Anthony M, Wright, John, and Chang, Shih-Fu. Learning with partially absorbing random walks. In *Advances in neural information processing systems*, pp. 3077–3085, 2012. 3
- [40] Wu, Xiao-Ming, Li, Zhenguang, and Chang, Shih-Fu. Analyzing the harmonic structure in graph-based learning. In *Advances in Neural Information Processing Systems*, pp. 3129–3137, 2013. 3
- [41] Wu, Zonghan, Pan, Shirui, Chen, Fengwen, Long, Guodong, Zhang, Chengqi, and Philip, S Yu. A comprehensive survey on graph neural networks. *IEEE Transactions on Neural Networks and Learning Systems*, 2020. 1
- [42] Xu, Bingbing, Shen, Huawei, Cao, Qi, Cen, Keting, and Cheng, Xueqi. Graph convolutional networks using heat kernel for semi-supervised learning. In *Proceedings of the 28th International Joint Conference on Artificial Intelligence*, pp. 1928–1934. AAAI Press, 2019. 3
- [43] Xu, Keyulu, Li, Chengtao, Tian, Yonglong, Sonobe, Tomohiro, Kawarabayashi, Ken-ichi, and Jegelka, Stefanie. Representation learning on graphs with jumping knowledge networks. *arXiv preprint arXiv:1806.03536*, 2018. 1, 2, 5, 7, 13, 14, 15
- [44] Yang, Zhilin, Cohen, William W, and Salakhutdinov, Ruslan. Revisiting semi-supervised learning with graph embeddings. *arXiv preprint arXiv:1603.08861*, 2016. 1, 3, 5, 7, 12, 13
- [45] Ying, Rex, He, Ruining, Chen, Kaifeng, Eksombatchai, Pong, Hamilton, William L, and Leskovec, Jure. Graph convolutional neural networks for web-scale recommender systems. In *Proceedings of the 24th ACM SIGKDD International Conference on Knowledge Discovery & Data Mining*, pp. 974–983, 2018. 3
- [46] Zhang, Jiani, Shi, Xingjian, Xie, Junyuan, Ma, Hao, King, Irwin, and Yeung, Dit-Yan. Gaan: Gated attention networks for learning on large and spatiotemporal graphs. *arXiv preprint arXiv:1803.07294*, 2018. 1, 2, 3
- [47] Zhang, Ziwei, Cui, Peng, and Zhu, Wenwu. Deep learning on graphs: A survey. *IEEE Transactions on Knowledge and Data Engineering*, 2020. 1
- [48] Zhou, Dengyong, Bousquet, Olivier, Lal, Thomas N, Weston, Jason, and Schölkopf, Bernhard. Learning with local and global consistency. In *Advances in neural information processing systems*, pp. 321–328, 2004. 1

- [49] Zhou, Jie, Cui, Ganqu, Zhang, Zhengyan, Yang, Cheng, Liu, Zhiyuan, Wang, Lifeng, Li, Changcheng, and Sun, Maosong. Graph neural networks: A review of methods and applications. *arXiv preprint arXiv:1812.08434*, 2018. 1
- [50] Zhu, Xiaojin, Ghahramani, Zoubin, and Lafferty, John D. Semi-supervised learning using gaussian fields and harmonic functions. In *Proceedings of the 20th International conference on Machine learning (ICML-03)*, pp. 912–919, 2003. 1

A Implementation

In this section, we present the detailed implementation of CAD-Net. We used PyTorch Geometric [9] for implementation. Table 2 summarizes a full list of hyperparameters of CAD-Net used in the experiments. For all datasets, 2-layers of MLP with the number of hidden units of 64 was used for f_θ . We used the leaky ReLU activation and dropout for the whole network. The number of diffusion steps K and the sensitivity β were determined empirically. We used the graphs with self-loops for CiteSeer and Cora because their graphs contain a number of isolated regions where only few nodes are connected. For training, we used Adam optimizer [17] with full-batch. During training, we dropped the learning rate to 1/2 of its previous value every 100 epochs (CiteSeer and PubMed) and 50 epochs (Cora). We also used L_2 regularization on the learnable parameters with weight decay of 0.0005. In addition, λ_{ent} denotes the weighting parameter for our entropy regularization loss term \mathcal{L}_{ent} . For Cora and PubMed, as in other works [18, 20, 38], we used early stopping with a window size of 10 and 30 respectively after half of the total epochs have passed. On the other hand, the performance was slightly better without early stopping for CiteSeer. We also submit demo files of CAD-Net for CiteSeer, Cora, and PubMed, including the source codes and the datasets, which reproduce the results under standard benchmark settings [44]. Our full code will be available after the publication.

Table 2: Hyperparameters for CAD-Net used in the experiments.

	CITESEER	CORA	PUBMED
layers	2	2	2
hidden units	64	64	64
leaky ReLU	0.05	0.05	0.1
dropout (p_{drop})	0.3	0.5	0.3
K	3	6	8
β	0.7	0.8	0.85
self-loop	o	o	-
epochs	200	100	300
initial learning rate (lr)	0.03	0.01	0.03
lr drop (epoch/drop rate)	100/0.5	50/0.5	100/0.5
weight decay	0.0005	0.0005	0.0005
λ_{ent}	0.3	0.5	0.5
early stop (window size)	-	10	30

B Experiment Details

B.1 Datasets

All datasets used in the experiments are included in PyTorch Geometric [9]. Dataset statistics are summarized in Table 3.

Table 3: Dataset statistics.

Dataset	#Nodes	#Edges	#Feature	#Classes	#Training	#Validation	#Test
CITESEER	3327	4552	3703	6	120	500	1000
CORA	2708	5278	1433	7	140	500	1000
PUBMED	19717	44324	500	3	60	500	1000

B.2 Results

Influence of β . Figure 6 shows the effect of the hyperparameter β which controls the sensitivity of how much γ will be adjusted. The blue line indicates the mean accuracy with different β and the shaded area indicates the standard deviation computed over 100 independent runs. The black dashed line indicates the existing state-of-the-art performance. While the optimum value for β differs slightly for each dataset, we can observe that any $\beta \in [0.65, 0.95]$ achieve the state-of-the-art performances. Note that setting $\beta = 1$ leads to $\gamma_i = 1$, which corresponds to CAD-only (blue dashed line) that only uses CAD without the adaptive aggregation in AggCAD. The CAD-only model achieves state-of-the-art performance for all datasets, demonstrating that the proposed CAD is effective. We further confirm that a proper β leads to additional performance gain (red dashed line) for all datasets. That is, by means of γ , the model can adjust the reflection ratio of the diffusion to prevent corrupted representations from inter-class neighbors, which leads to better performance. Figure 7 illustrates the distribution of the resulting γ values for entire nodes.

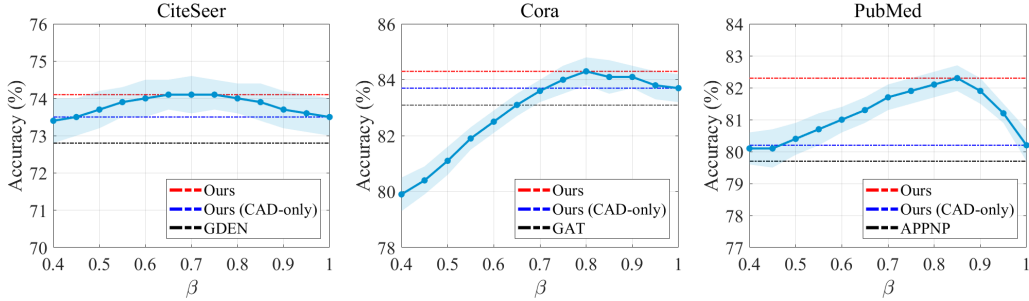


Figure 6: Accuracy with different β . For all datasets, $\beta \in [0.65, 0.95]$ consistently achieves the state-of-the-art performances.

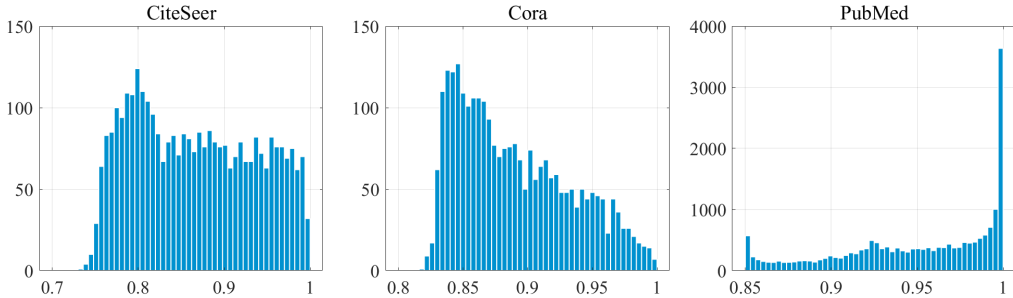


Figure 7: Histogram of γ values for each dataset. Different datasets exhibit different distributions.

Influence of Different Label Rates. From the given training set by the benchmark setting [44] where 20 nodes per class are labeled, we randomly reduced the number of labeled nodes per class to 15, 10, and 5. Table 4, 5, and 6 show detailed results illustrated in Figure 4 of the manuscript.

Influence of Different Ranges. For Cheby [8], we used K -th order of Chebyshev polynomials to meet the range of K . For GCN [18], SAGE [13], JK [43], and GAT [37], we added additional layers before the last layer to achieve the desired range, whereas, for SGC [38], AGNN [35], APPNP [35], and the proposed CAD-Net, we simply increased the propagation steps. Table 7, 8, and 9 show detailed results illustrated in Figure 5 of the manuscript.

Table 4: Accuracy (%) on CITESEER with different numbers of labeled nodes per class. The following tables show detailed results illustrated in Figure 4 of the manuscript. We report the mean with the standard deviation (Mean \pm Std) computed over 100 independent runs. The best results are marked by bold.

Method	Labeled nodes per class			
	5	10	15	20
Cheby [8]	58.4 \pm 1.3	70.3 \pm 0.5	70.9 \pm 0.6	70.7 \pm 0.5
GCN [18]	57.1 \pm 2.5	68.3 \pm 1.1	71.1 \pm 0.8	71.1 \pm 0.7
SAGE [13]	60.1 \pm 1.8	69.2 \pm 0.7	70.9 \pm 0.6	70.9 \pm 0.7
JK [43]	59.8 \pm 1.5	63.6 \pm 2.0	69.6 \pm 0.9	69.2 \pm 0.9
MixHop [2]	62.9 \pm 1.3	69.1 \pm 1.1	70.8 \pm 1.1	71.5 \pm 0.8
SGC [38]	61.6 \pm 0.2	68.5 \pm 0.2	71.6 \pm 0.1	71.9 \pm 0.1
AGNN [35]	62.0 \pm 2.0	70.1 \pm 0.9	71.3 \pm 0.8	71.5 \pm 0.7
GAT [37]	64.4 \pm 1.6	70.1 \pm 0.8	71.9 \pm 0.9	72.5 \pm 0.8
U-Nets [10]	60.8 \pm 1.4	68.1 \pm 0.9	69.9 \pm 0.7	70.2 \pm 1.5
APPNP [19]	63.0 \pm 1.3	70.5 \pm 0.7	71.9 \pm 0.5	71.8 \pm 0.5
GDC [20]	64.3 \pm 1.6	70.1 \pm 0.9	71.5 \pm 0.8	72.7 \pm 0.8
Proposed	67.7 \pm 1.1	72.2 \pm 0.7	73.9 \pm 0.5	74.1 \pm 0.4

Table 5: Accuracy (%) on CORA with different numbers of labeled nodes per class.

Method	Labeled nodes per class			
	5	10	15	20
Cheby [8]	59.9 \pm 2.5	70.9 \pm 1.7	79.6 \pm 0.6	81.4 \pm 0.5
GCN [18]	69.6 \pm 1.6	74.8 \pm 1.1	80.1 \pm 0.9	81.3 \pm 0.7
SAGE [13]	71.0 \pm 1.6	75.9 \pm 1.1	80.2 \pm 0.7	81.4 \pm 0.7
JK [43]	69.8 \pm 1.7	73.5 \pm 1.3	79.4 \pm 1.0	81.2 \pm 0.8
MixHop [2]	72.7 \pm 1.5	76.2 \pm 1.2	80.6 \pm 0.9	82.0 \pm 0.8
SGC [38]	70.8 \pm 0.1	74.7 \pm 0.1	78.2 \pm 0.1	81.0 \pm 0.2
AGNN [35]	74.0 \pm 1.2	78.4 \pm 0.8	82.1 \pm 0.8	82.8 \pm 0.6
GAT [37]	73.8 \pm 0.7	78.6 \pm 0.6	82.5 \pm 0.5	83.1 \pm 0.8
U-Nets [10]	73.6 \pm 1.8	76.8 \pm 1.4	81.4 \pm 0.9	82.9 \pm 0.7
APPNP [19]	73.9 \pm 0.9	77.5 \pm 0.8	82.2 \pm 0.5	82.9 \pm 0.5
GDC [20]	74.9 \pm 1.1	78.6 \pm 0.9	81.7 \pm 0.8	82.7 \pm 0.7
Proposed	76.7 \pm 1.2	80.5 \pm 0.7	83.8 \pm 0.6	84.3 \pm 0.5

Table 6: Accuracy (%) on PUBMED with different numbers of labeled nodes per class.

Method	Labeled nodes per class			
	5	10	15	20
Cheby [8]	65.1 \pm 1.5	71.1 \pm 1.6	72.0 \pm 1.9	75.2 \pm 1.4
GCN [18]	67.5 \pm 1.0	75.2 \pm 0.6	77.9 \pm 0.5	79.0 \pm 0.5
SAGE [13]	68.8 \pm 1.0	74.8 \pm 0.7	77.7 \pm 0.6	78.7 \pm 0.4
JK [43]	70.3 \pm 1.2	75.1 \pm 0.6	78.1 \pm 0.4	78.8 \pm 0.5
MixHop [2]	69.1 \pm 2.0	76.0 \pm 1.0	78.8 \pm 0.6	79.6 \pm 0.4
SGC [38]	66.1 \pm 0.5	73.9 \pm 0.2	76.7 \pm 0.1	78.9 \pm 0.1
AGNN [35]	68.2 \pm 1.1	74.4 \pm 0.7	78.5 \pm 0.7	79.3 \pm 0.8
GAT [37]	67.3 \pm 1.0	74.3 \pm 0.7	78.5 \pm 0.4	79.0 \pm 0.3
U-Nets [10]	69.7 \pm 1.1	74.6 \pm 0.7	78.2 \pm 0.5	77.9 \pm 0.9
APPNP [19]	69.4 \pm 0.9	77.3 \pm 0.5	79.3 \pm 0.5	79.7 \pm 0.3
GDC [20]	68.2 \pm 1.0	72.3 \pm 0.4	77.5 \pm 0.4	78.1 \pm 0.3
Proposed	77.1 \pm 1.4	78.9 \pm 1.5	81.5 \pm 0.4	82.3 \pm 0.4

Table 7: Accuracy (%) on CITESEER with varying ranges of the model. The following tables show detailed results illustrated in Figure 5 of the manuscript. We report the mean with the standard deviation (Mean \pm Std) computed over 100 independent runs. The best results are marked by bold.

Method	Range (hop)				
	2	4	6	8	10
Cheby [8]	70.7 \pm 0.5	65.6 \pm 1.9	60.8 \pm 4.1	56.6 \pm 5.1	56.8 \pm 3.9
GCN [18]	71.1 \pm 0.7	58.4 \pm 5.9	35.0 \pm 9.6	24.5 \pm 7.2	21.3 \pm 2.3
SAGE [13]	70.9 \pm 0.7	36.1 \pm 7.7	19.1 \pm 2.5	18.4 \pm 2.2	19.2 \pm 2.7
JK [43]	69.1 \pm 1.1	65.1 \pm 1.7	63.8 \pm 1.8	64.3 \pm 2.1	63.6 \pm 2.4
SGC [38]	71.9 \pm 0.1	70.8 \pm 0.1	71.2 \pm 0.1	71.2 \pm 0.3	71.3 \pm 0.2
AGNN [35]	70.9 \pm 0.9	71.5 \pm 0.7	71.4 \pm 0.8	71.2 \pm 0.8	71.0 \pm 0.7
GAT [37]	72.5 \pm 0.8	66.7 \pm 1.6	62.0 \pm 4.4	59.2 \pm 4.7	51.2 \pm 10.2
APPNP [19]	72.0 \pm 0.7	71.8 \pm 0.5	71.6 \pm 0.5	71.7 \pm 0.5	71.7 \pm 0.5
Proposed	73.8 \pm 0.4	74.0 \pm 0.5	73.7 \pm 0.5	73.7 \pm 0.5	73.7 \pm 0.5

Table 8: Accuracy (%) on CORA with varying ranges of the model.

Method	Range (hop)				
	2	4	6	8	10
Cheby [8]	81.4 \pm 0.5	78.5 \pm 1.7	71.7 \pm 5.7	62.1 \pm 9.9	57.1 \pm 10.4
GCN [18]	81.3 \pm 0.7	74.2 \pm 4.0	49.0 \pm 15.7	20.3 \pm 8.8	20.8 \pm 8.6
SAGE [13]	81.4 \pm 0.7	51.3 \pm 13.9	20.5 \pm 9.1	20.6 \pm 9.6	22.1 \pm 10.1
JK [43]	81.2 \pm 0.8	79.3 \pm 1.1	78.7 \pm 1.7	78.4 \pm 1.6	78.3 \pm 2.2
SGC [38]	81.0 \pm 0.2	81.0 \pm 0.3	80.6 \pm 0.4	80.4 \pm 0.4	80.5 \pm 0.4
AGNN [35]	82.8 \pm 0.6	81.7 \pm 0.7	81.5 \pm 0.7	81.4 \pm 0.6	81.3 \pm 0.5
GAT [37]	83.1 \pm 0.8	80.5 \pm 1.3	76.6 \pm 2.5	75.4 \pm 2.4	74.8 \pm 2.8
APPNP [19]	81.2 \pm 0.6	81.2 \pm 0.6	82.2 \pm 0.8	82.2 \pm 0.9	82.0 \pm 0.9
Proposed	82.5 \pm 0.5	83.8 \pm 0.4	84.3 \pm 0.5	84.2 \pm 0.4	83.8 \pm 0.5

Table 9: Accuracy (%) on PUBMED with varying ranges of the model.

Method	Range (hop)				
	2	4	6	8	10
Cheby [8]	75.2 \pm 1.4	72.6 \pm 3.4	69.8 \pm 3.4	70.0 \pm 4.7	71.5 \pm 5.3
GCN [18]	79.0 \pm 0.5	75.0 \pm 3.9	65.0 \pm 9.9	43.7 \pm 2.8	39.4 \pm 1.0
SAGE [13]	78.7 \pm 0.4	66.4 \pm 9.2	41.8 \pm 3.4	41.0 \pm 0.3	41.0 \pm 0.3
JK [43]	78.7 \pm 0.5	75.8 \pm 1.8	74.7 \pm 2.6	74.9 \pm 2.3	75.3 \pm 2.1
SGC [38]	78.9 \pm 0.1	79.4 \pm 0.1	77.7 \pm 0.2	77.1 \pm 0.4	75.9 \pm 0.3
AGNN [35]	78.9 \pm 0.6	79.3 \pm 0.8	77.9 \pm 0.6	77.2 \pm 0.6	76.7 \pm 0.5
GAT [37]	79.0 \pm 0.3	74.6 \pm 4.1	73.1 \pm 4.6	73.3 \pm 6.0	73.0 \pm 3.3
APPNP [35]	79.3 \pm 0.3	79.7 \pm 0.3	80.1 \pm 0.3	80.1 \pm 0.2	80.2 \pm 0.3
Proposed	79.2 \pm 0.7	81.3 \pm 0.5	82.0 \pm 0.4	82.3 \pm 0.4	81.9 \pm 0.3